January 9-13, 2000 Hong Kong

Proceedings of

Symposium on Energy Engineering in the 21st Century (SEE 2000)

Volume One

Begell House New York, Wallingford (U.K.)

Ping Cheng Editor

Proceedings

of

Symposium on Energy Engineering in the 21st Century (SEE2000)

Volume 1

Edited by

Ping Cheng
Mechanical Engineering Department
The Hong Kong University of Science and Technology
Clear Water Bay, Kowloon, Hong Kong

Begell House
New York, Wallingford (U.K.)

Library of Congress Cataloging-in-Publication Data

Catalog record is available from the Library of Congress.

This book represents information obtained from authentic and highly regarded sources. Reprinted material is quoted with permission, and sources are indicated. A wide variety of references are listed. Every reasonable effort has been made to give reliable data and information, but the authors and the publisher cannot assume responsibility for the validity of all materials or for the consequences of their use.

Direct all inquiries to Begell House, Inc., 79 Madison Avenue, New York, NY 10016.

ISBN 1-56700-132-7 (hard cover edition)

Printed in Hong Kong 1 2 3 4 5 6 7 8 9 0

FORWARD

The signing of the Montreal Protocol in 1987 and the Kyoto Protocol in 1997 by various nations serves as a reminder once again of the intimate relationship between energy and environment, which will no doubt remain one of the major issues in the 21st Century. This is particularly so in Southeast Asia, where industrial growth has taken place at such a rapid pace during the last two decades. At the same time, research in energy engineering is accelerating in this part of the world. At the Hong Kong University of Science and Technology (HKUST), the Center for Energy and Thermal Systems (CETS) was recently established for the research and development of energy efficient and environmentally benign thermal systems. Thus, it is a privilege for CETS to be able to host the Symposium on Energy Engineering in the 21st Century (SEE2000) on the HKUST campus between 9-13 January 2000, the first international energy engineering conference ever held in Hong Kong.

The aim of this Symposium is to provide a forum for technical interchange in various aspects of energy engineering. The 226 papers (including 11 keynote papers) presented in the 25 technical sessions of the Symposium are published in this proceedings which contains 4 volumes, covering a variety of topics from heat and mass transfer, various energy and thermal systems, to clean combustion technology.

It has been a great pleasure for me to work with Symposium Co-Chairmen Professor Kefa Cen of the Zhejiang University and Professor Patrick Takahashi of the University of Hawaii in the planning of this Symposium. I would like to express my sincere thanks to keynote speakers for their efforts in writing up-to-date review papers, to members of the International Advisory Committee and the Organizing Committee for their enthusiasm in promoting the Symposium, and to members of the Local Committee for their hard work in reviewing the manuscripts. Special thanks are due to Dr. H. H. Qiu (the Symposium Secretariat) and Ms. Lotta Tse for their help in making conference arrangements, as well as to Ms. Ellie Ho, Ms. Ronnie Tse and other clerical staff for their help in the typing of the manuscripts and for the preparation of the proceedings. The generous financial support from the K. C. Wong Education Foundation, U.S. Air Force Asian Office of Aerospace Research and Development, U.S. Army Research Office - Far East, U.S. Office of Naval Research - Asia, and the International Technic HVAC Company are gratefully acknowledged.

Ping Cheng
Symposium Chair

Hong Kong
January 2000

SYMPOSIUM CHAIRMAN

Professor Ping Cheng
Department of Mechanical Engineering
Hong Kong University of Science and Technology
Clear Water Bay, Kowloon, Hong Kong
Fax: (852) 2358-1543 E-mail: mepcheng@ust.hk

SYMPOSIUM CO-CHAIRMEN

Professor Kefa Cen
Institute for Thermal Power Engineering
Zhejiang University
Hangzhou 310027, China
Fax: (86) 571-595-1616
E-mail: kfcen@sun.zju.edu.cn

Professor Patrick Takahashi
Hawaii Natural Energy Institute
University of Hawaii
Honolulu, Hawaii 96822, U.S.A.
Fax: (808) 956-2336
E-mail: ptakaha@uhccmvs.uhcc.hawaii.edu

SYMPOSIUM SECRETARIAT

Dr. H. H. Qiu
Department of Mechanical Engineering
Hong Kong University of Science and Technology
Clear Water Bay, Kowloon, Hong Kong
Fax: (852) 2358-1543 E-mail: meqiu@ust.hk

INTERNATIONAL ADVISORY COMMITTEE

ORGANISING COMMITTEE

Auracher, H. L., Technical University of Berlin, Berlin
Cai, R. X., Institute of Engineering Thermophysics, Beijing
Chen, T. S., University of Missouri, Rolla
Faghri, A., University of Connecticut, Storrs
Fujii, T., Kobe University, Kobe
Fukusako, S., Hokkaido University, Sapporo
Groll, M., University of Stuttgart, Stuttgart
Guo, Z. Y., Tsinghua University, Beijing
Howell J., University of Texas, Austin
Inaba, H., Okayama University, Okayama
Kakac, S., University of Miami, Miami
Kashiwagi, T., Tokyo University of Agriculture & Technology, Tokyo
Kaviany, M., University of Michigan, Ann Arbor
Kennedy, L. A., The University of Illinois at Chicago, Chicago
Kim, Jong Hyun, EPRI, Palo Alto
Kurosaki, Y., University of Electro-Communications, Tokyo
Law, C. K., Princeton University, Princeton
Lee, J. S., Seoul National University, Seoul
Lloyd, A. C., Desert Research Institute, Reno
Lou, D. Y. S., University of Nebraska, Lincoln
Minkowycz, W. J., University of Illinois at Chicago, Chicago
Nelson, R. A., Los Alamos National Laboratory, Los Alamos
Ni, M. J., Zhejiang University, Hangzhou
Nishio, S., University of Tokyo, Tokyo
Peng, X. F., Tsinghua University, Beijing
Peterson, G. P., Texas A & M University, College Station
Radebaugh, R., National Institute of Standards and Technology, Boulder
Saitoh, T. S., Tohoku University, Sendai
Serizawa, A., Kyoto University, Kyoto
Shoji, M., University of Tokyo, Tokyo
Son, J. E., Korea Institute of Energy Research, Taejon
Straub, J., Technical University of Munich, Munich
Suzuki, K., Kyoto University, Kyoto
Tong, T. W., Colorado State University, Fort Collins
Wang, C. Y., Pennsylvania State University, College Park

LOCAL COMMITTEE

Hsu, C. T, HKUST
Chao, Y. H., HKUST
Chi, Y, Zhejiang University
Kot, S. C., HKUST
Lee, H. K., HKUST
Qiu, H. H., HKUST
Zhao, T. S., HKUST.

SPONSORS

American Society of Mechanical Engineers
Japanese Society of Mechanical Engineers
Chinese Society of Power Engineering
International Center of Heat and Mass Transfer
K. C. Wong Education Foundation
U.S. Air Force Asian Office of Aerospace Research and Development
U.S. Army Research Office-Far East
U.S. Office of Navy Research-Asia

SUMMARY OF TECHNICAL SESSIONS

Volume 1

A. Keynote Papers
B. Forced Convection
C. Natural Convection
D. Boiling and Condensation

Volume 2

E. Two-Phase Flow
F. Porous Media
G. Heat Pipes and Thermosyphons
H. Conduction and Radiation
I. Microscale Heat Transfer
J. Heat Transfer Enhancement
K. Solar Energy & Nuclear Energy
L. Thermal Storage
M. Melting and Solidification

Volume 3

N. Drying and Food Processing
O. Heat Exchangers
P. Air-Conditioning and Refrigeration
Q. Cryogenic Engineering
R. Energy and Environment
S. Combustion and Fire

Volume 4

T. Cycle Analysis
U. Engine Combustion
V. Waste Treatment by Thermal Methods
W. Fuel Cells
X. Clean Combustion Technology
Y. Coal Combustion

CONTENTS OF VOLUME 1

A. Keynote Papers

HYBRID THERMOACOUSTIC-STIRLING ENGINES AND REFRIGERATORS

G. W. Swift
Condensed Matter and Thermal Physics Group
Los Alamos National Laboratory
Los Alamos NM 87545 USA
Email: swift@lanl.gov; Fax: 505-665-7652

Keywords: Stirling engine, Stirling refrigerator, acoustics, thermoacoustics

ABSTRACT. The use of thermoacoustic principles to eliminate all moving parts from Stirling engines and refrigerators leads to devices with the inherently high efficiency of the Stirling cycle and the simplicity of no moving parts. We have demonstrated over 40% of the Carnot efficiency in such a device; higher efficiency appears to be possible. The gas dynamics resembles that of free-piston Stirling devices, but with gas inertia playing the role of piston masses. However, large time-averaged flows can be superimposed on the oscillating flows. Control of the time-averaged flows is essential to ensure that they do not reduce efficiency by convecting significant amounts of heat.

1. INTRODUCTION

The typical Stirling engine of a century ago had many moving parts: crankshafts, connecting rods, pistons. The mechanical parts dominated the thermal parts—in volume, weight, and visual impact—in these machines. Since then, engineers have sought to simplify such machines by elimination of moving parts. Eliminating connecting rods and crankshafts produced free-piston [1,2] Stirling engines and refrigerators, in which the moving pistons bounce against gas "springs" in resonance. The liquid-piston Stirling engine [3], in which liquid in two U tubes serves the function of the two pistons of the ordinary Stirling engine, also eliminates moving parts.

Ceperley [4,5] realized that the phasing between pressure and velocity in the heat exchangers of Stirling devices is the same as that in a traveling acoustic wave, so he proposed eliminating everything but the working gas itself, using acoustics to control the gas motion and gas pressure. Ceperley's work showed the need to consider sound-wave behavior in the working gas of Stirling devices, with variations in important variables such as pressure and velocity depending strongly and continuously on the coordinate x along the direction of gas motion, and with these x dependences due to inertial and compressive effects in the gas in addition to the effects of flow resistance.

We have recently built a hybrid thermoacoustic-Stirling engine [6,7] and a hybrid thermoacoustic-Stirling refrigerator [8], combining Ceperley's ideas with a modern thermoacoustic perspective [9]. This manuscript is only an introduction to such hybrids; details can be found in the references.

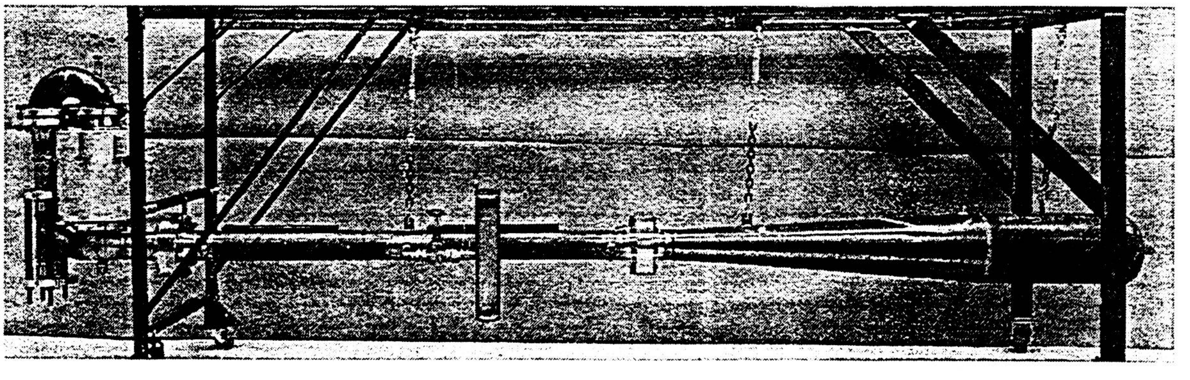

Fig. 1: A hybrid thermoacoustic-Stirling heat engine for research.

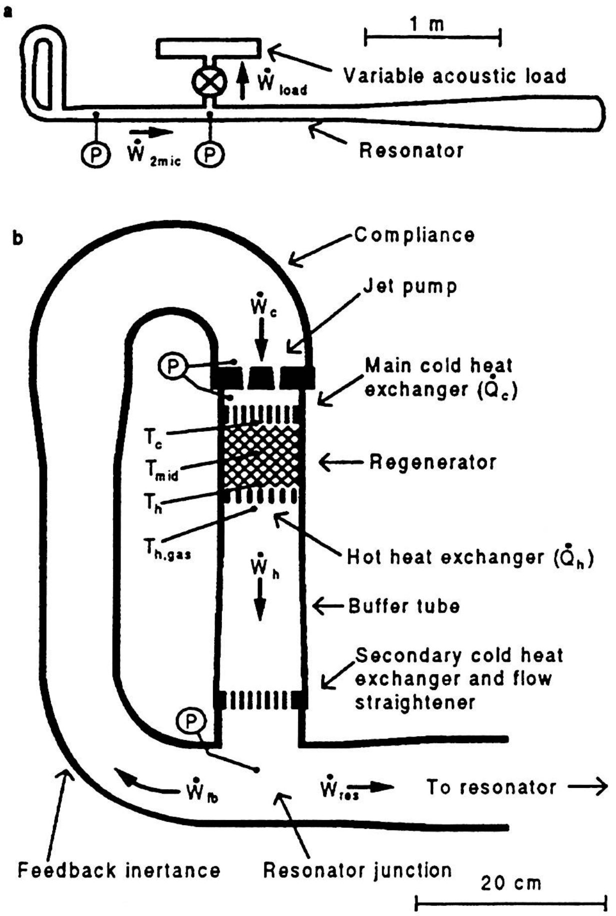

Fig. 2: The hybrid thermoacoustic-Stirling engine. (a) Overview, as in the photo. (b) The heart of the engine. The two heat exchangers labeled "cold" are held at ambient temperature by flowing water.

2. EXAMPLES

Example: Acoustic-Stirling heat engine. In the heat engine [6,7] shown in **Figs. 1** and **2**, heat was supplied to the engine electrically, and waste heat was removed by a water stream; the engine delivered up to 890 W of acoustic power to the resonator. Some of that acoustic power was dissipated in the resonator, but most was delivered to a variable acoustic load, the small vertical cylinder near the center of **Fig. 1**. This engine has delivered 710 W of acoustic power to the resonator with an efficiency equal to 42% of the Carnot efficiency. (Here, efficiency is acoustic power delivered to the resonator to the right of the junction, divided by electric power supplied to the engine's heater, and the temperatures used in the Carnot factor are those of the gas just below the hot heat exchanger and of the engine's cooling water.) Suppression of steady flow around the small torus containing the heat exchangers is crucial for this high efficiency, as we will discuss below. Thirty-bar helium filled the system, oscillating at 80 Hz. The resonator is essentially half-wavelength, with pressure oscillations 180° out of phase at the right end of the fat portion on the right and in the small torus containing the heat exchangers on the left. The highest velocity occurs in the center of the resonator, at the small end of the long cone.

The key idea in this and other Stirling engines is that the gas in the regenerator experiences thermal expansion when the pressure is high and thermal contraction when the pressure is low. Thus the gas in the regenerator does work every cycle, pumping acoustic power into the sound wave. The sound wave in turn provides two things: oscillating pressure, and oscillating motion that causes the gas in the regenerator to experience the oscillating temperature responsible for the thermal expansion and

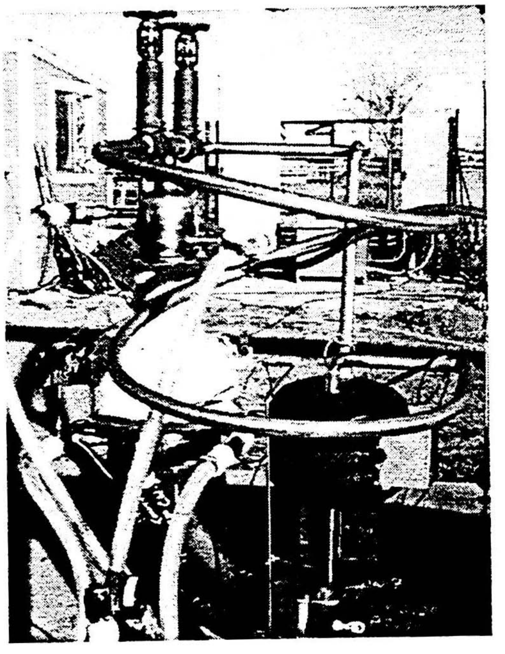

Fig. 3: The Cryenco 2-kW orifice pulse-tube refrigerator.

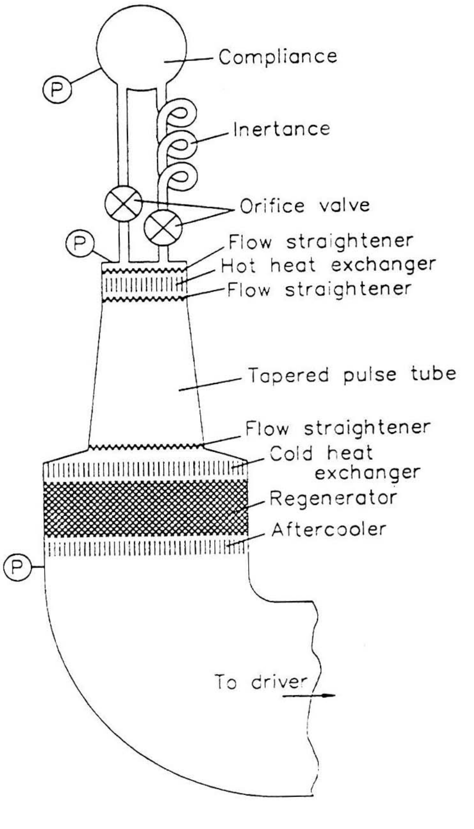

Fig. 4: Schematic of the Cryenco orifice pulse-tube refrigerator. "P" indicates the location of a pressure sensor. Ambient-temperature water flows through the "hot" heat exchanger and aftercooler. The regenerator diameter is approximately 20 cm.

contraction. These complex, coupled oscillations appear spontaneously whenever the temperature at the hot end of the regenerator is high enough. The velocity of the gas along the regenerator's temperature gradient is substantially in phase with the oscillating pressure, so good thermal contact between gas and regenerator is required to cause the thermal expansion and contraction steps to be in phase with the oscillating pressure. This thermal contact is achieved by making the channel size in the regenerator much smaller than the thermal penetration depth.

Example: Orifice pulse-tube refrigerator. The orifice pulse-tube refrigerator shown in **Figs. 3** and **4** was built by Cryenco for liquefaction of natural gas [10,11]. At about 3 bar, natural gas (methane) liquefies at 120 Kelvin; this refrigerator provided 2 kW of refrigeration at that temperature, with a COP as high as 23% of the Carnot COP. (Here, the coefficient of performance COP is the heat removed from the methane stream divided by the acoustic power incident on the aftercooler from below, and the temperatures used in the Carnot factor are those of the liquefied methane and of the cooling water.) The working gas was helium at a pressure of thirty atmospheres, driven at 40 Hz by a thermoacoustic engine through a resonator, not shown in the figures.

The key idea in this and other Stirling, pulse-tube, and hybrid refrigerators is that gas near the cold heat exchanger must be displaced into the open space away from the regenerator, adiabatically cooled, and displaced back through the cold heat exchanger where it can absorb heat from the load. The wave must provide oscillating pressure and oscillating displacement with this required phasing.

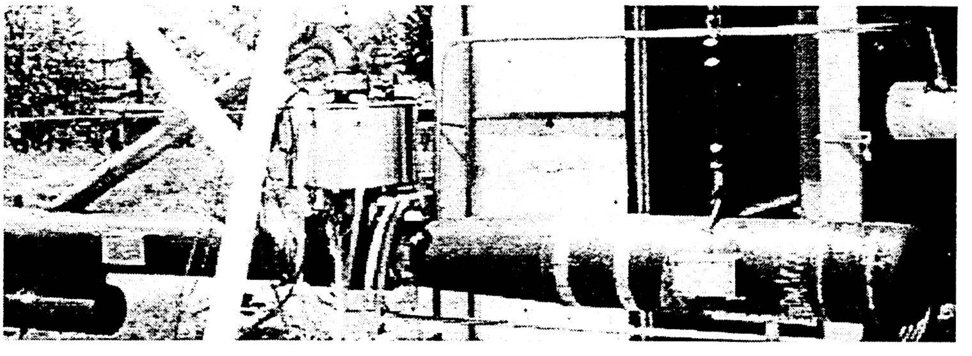

Fig. 5: A hybrid acoustic-Stirling refrigerator. A cylindrical stainless-steel vacuum jacket hides the regenerator and pulse tube, which are similar in size to those of the refrigerator in Fig. 3. The 10-cm-diam pipe recovers acoustic power from the top of the pulse tube.

Example: Acoustic-Stirling refrigerator. The refrigerator described in Ref. [8] illustrates many of the principles of hybrid thermoacoustic-Stirling refrigeration, but had unimpressive overall performance. The refrigerator shown in **Fig. 5** was recently built at Cryenco [10] according to these principles, and should have comparable cooling power and higher COP than the orifice pulse-tube refrigerator of **Fig. 3**, but measurements have not been completed as of the writing of this manuscript.

3. THE THERMOACOUSTIC PERSPECTIVE

Waves

In the thermoacoustic perspective [9], the momentum equation shows how oscillations in velocity are coupled to spatial gradients in oscillating pressure, and the continuity equation shows how oscillations in pressure are coupled to spatial gradients in oscillating velocity. Throughout, we assume monofrequency, steady, "small" oscillations—an approximation that we refer to simply as "the acoustic approximation." Ordinarily we think of sound waves as *small* coupled oscillations of pressure and velocity: Even a painfully loud sound, such as 120 dB re 20 μPa, is a "small" oscillation, because $|p_1| \sim 0.0002 p_m$. Fortunately, the thermoacoustic approach remains reasonably accurate even for the "large" oscillations encountered in hybrid thermoacoustic-Stirling engines and refrigerators, typically $|p_1| \sim 0.1 p_m$, with $|p_1| > 10^5$ Pa.

We assume that all time dependence is purely sinusoidal, at frequency f and angular frequency $\omega = 2\pi f$. Then variables such as pressure p *could* be written

$$p(x,t) = p_m + C(x)\cos[\omega t + \phi(x)]\,. \tag{1}$$

It is much more convenient to rewrite Eq. (1) as

$$p(x,t) = p_m + \mathrm{Re}\left[p_1(x)e^{i\omega t}\right], \tag{2}$$

where $p_1(x)$ is a complex function of x such that

$$|p_1(x)| = C(x) \qquad \text{and} \qquad \mathrm{phase}[p_1(x)] = \phi(x). \tag{3}$$

This nòtation is preferred because a single symbol (with subscript 1) stands for both amplitude and phase, and because all the shortcuts of complex arithmetic can be used.

Hence, the thermoacoustic approach to Stirling engines and refrigerators writes the relevant variables as

$$\text{pressure } p = p_m + \mathrm{Re}\left[p_1(x)e^{i\omega t}\right], \tag{4}$$

$$\text{volume flow rate } U = \mathrm{Re}\left[U_1(x)e^{i\omega t}\right], \tag{5}$$

$$x \text{ component of velocity } u = \mathrm{Re}\left[u_1(x,y,z)e^{i\omega t}\right], \tag{6}$$

$$\text{temperature } T = T_m(x) + \mathrm{Re}\left[T_1(x,y,z)e^{i\omega t}\right], \tag{7}$$

$$\text{density } \rho = \text{similar to } T\,, \tag{8}$$

$$\text{viscosity } \mu = \mu(x)\,, \tag{9}$$

$$\text{thermal conductivity } k, \text{ etc.} = \text{similar to } \mu. \tag{10}$$

We are most interested in p_1 and U_1, as described by the momentum and continuity equations. The acoustic approximation to the x-component of the momentum equation is

$$i\omega\rho_m u_1 = -\frac{dp_1}{dx} + \mu\left[\frac{\partial^2 u_1}{\partial y^2} + \frac{\partial^2 u_1}{\partial z^2}\right]. \tag{11}$$

Regarding Eq. (11) as a differential equation for $u_1(y,z)$, with boundary condition $u_1 = 0$ at the solid surface, obtaining that solution, and integrating it with respect to y and z over the cross-sectional area A of the channel, we obtain the volume flow rate U_1. Solving this result for dp_1 yields

$$dp_1 = -\frac{i\omega\rho_m\,dx/A}{1-f_\nu}U_1, \tag{12}$$

where f_ν is a geometry-dependent function shown in **Fig. 6.** In effect, we regard this approximation to the momentum equation as the origin of pressure gradient in thermoacoustics: The motion U_1 of the gas causes the pressure gradient. The function f_ν is known for many geometries: boundary-layer approximation [12], parallel plates [13], circular pores [13], rectangular channels [14], the spaces between pins oriented along the direction of acoustic oscillations and arranged in a triangular array [15], and (to some extent) in the important case of screen beds [16].

In the same way that the momentum equation leads to Eq. (12), the equations of state, heat transfer, and continuity lead to.

$$dU_1 = -\frac{i\omega A\,dx}{\gamma p_m}[1+(\gamma-1)f_\kappa]\,p_1 + \frac{(f_\kappa - f_\nu)}{(1-f_\nu)(1-\sigma)}\frac{dT_m}{T_m}U_1, \tag{13}$$

where $\gamma = c_p/c_V$ is the specific-heat ratio and $\sigma = \mu c_p/k$ is the Prandtl number. We regard this approximation to the continuity equation as the origin of gradients in volume flow rate in thermoacoustics.

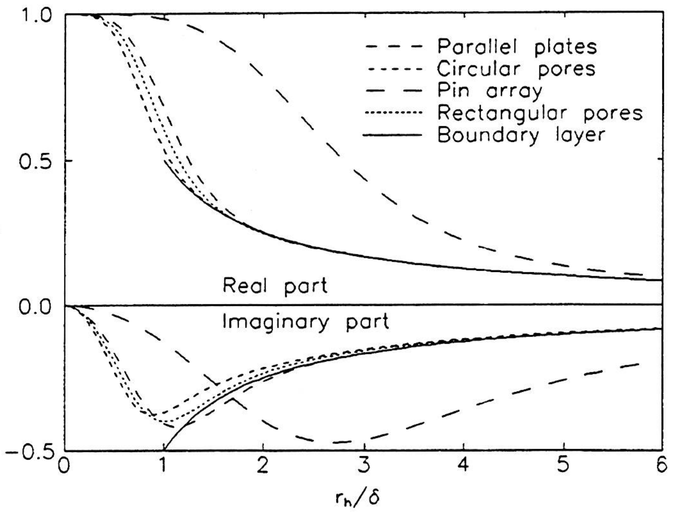

Fig. 6: Thermoacoustic spatial-average function f for several geometries. The hydraulic radius r_h is the ratio of cross-sectional area to perimeter, and the penetration depth δ is either the viscous penetration depth $\delta_\nu = \sqrt{2\mu/\omega\rho}$ or the thermal penetration depth $\delta_\kappa = \sqrt{2k/\omega\rho c_p}$. The rectangle has 6:1 aspect ratio, and the pin array has $r_o/r_i = 6$. The boundary-layer limit is approached at large r_h in all geometries.

Equations (12) and (13) are applicable to a wide variety of circumstances, and may be considered two of the principal tools of thermoacoustic analysis. To gain intuitive appreciation of these two equations, we can follow the outline indicated in **Fig. 7.** In the figure, a channel of length dx is considered in two ways: in terms of the momentum equation to obtain its inertance and viscous resistance, and in terms of the continuity equation to obtain its compliance, thermal-relaxation resistance, and thermally induced volume-flow-rate source. Combining these two points of view yields a complete impedance picture for thermoacoustics.

If we rewrite Eq. (12) in the form

$$dp_1 = -\left(i\omega l\, dx + r_\nu\, dx\right) U_1, \tag{14}$$

as shown schematically in the left part of **Fig. 7**, then the inertance, l, and the viscous resistance, r_ν, per unit length of channel can be written

$$l = \frac{\rho_m}{A}\frac{1-\mathrm{Re}\left[f_\nu\right]}{\left|1-f_\nu\right|^2} \qquad \text{and} \qquad r_\nu = \frac{\omega\rho_m}{A}\frac{\mathrm{Im}\left[-f_\nu\right]}{\left|1-f_\nu\right|^2}. \tag{15}$$

These expressions show how the pressure gradient in a duct arises from inertial and viscous effects. Similarly, Eq. (13) can be rewritten in the form

$$dU_1 = -\left(i\omega c\, dx + \frac{1}{r_\kappa}dx\right)p_1 + e\, dx\, U_1, \tag{16}$$

as shown schematically in the right part of **Fig. 7**. The compliance per unit length c and the thermal-relaxation conductance per unit length $1/r_\kappa$ are given by

$$c = \frac{A}{\gamma p_m}\left(1+\left[\gamma-1\right]\mathrm{Re}\left[f_\kappa\right]\right) \qquad \text{and} \qquad \frac{1}{r_\kappa} = \frac{\gamma-1}{\gamma}\frac{\omega A\ \mathrm{Im}\left[-f_\kappa\right]}{p_m}. \tag{17}$$

These expressions show that a gradient in U_1 can be caused either by pressure or by flow along the temperature gradient. Consider the compliance first. If $f_\kappa = 0$, there is no thermal contact between gas and solid, so the density oscillations are adiabatic; in this case, $1/\gamma p_m$ is the correct compressibility, and